



Joining of the alloys AA1050 and AA5754—Experimental characterization and multiscale modeling based on a cohesive zone element technique



R. Kebriaei*, I.N. Vladimirov, S. Reese

RWTH Aachen University, Institute of Applied Mechanics, Mies-van-der-Rohe-Str. 1, D-52074 Aachen, Germany

ARTICLE INFO

Article history:

Received 19 August 2013

Received in revised form 6 March 2014

Accepted 8 March 2014

Available online 15 March 2014

Keywords:

Chemo-mechanical characterization

Cohesive zone element formulation

Crystal plasticity

Roll bonding

ABSTRACT

The microstructure of two widely used engineering materials is experimentally and numerically investigated. Experimental measurements at the macroscopic scale are used for the validation of the micromechanical crystal plasticity computations. A major point of the paper is the development of a cohesive zone element formulation in the framework of zero-thickness interface elements. This enables the realistic modeling of bonding and debonding based on a traction-separation law. The ability of the cohesive zone element in describing the interface behavior is illustrated by means of several numerical examples, including the process of roll bonding.

© 2014 Elsevier B.V. All rights reserved.

1. Introduction

The roll bonding process is used to manufacture metal composites with improved mechanical properties by joining similar or dissimilar materials together (see Fig. 1). Typical applications can be found in aerospace, automotive and building industries as well as nuclear industries. An overview of the state of the art in joining processes as well as the potential of a novel manufacturing process for bonding of metallic sheets were presented by Mori et al. (2013). The joined structures are produced in different geometric form such as e.g. plate, strip, foil, tube, rod and wire shapes. Joining of dissimilar foils and strips using shot peening was proposed by Harada et al. (1998). Weddeling et al. (2011) discussed the process chain of forming, cutting and joining for the flexible production of lightweight structures. Schäfer et al. (2013) investigated new joining techniques for building industries. The authors studied several techniques such as e.g. flow-splitting and bend-splitting to create an ultra-fine grained microstructure in the formed flange.

Bay (1979) discussed the improved mechanisms for mechanical welding of metallic layers. Following these investigations, Bay (1989) introduced a numerical model which describes the behavior of bonding strength in cold roll bonding processes. In comparison

with alternative methods (e.g. self-pierce riveting, mechanical clinching and hydroforming) roll bonding has several advantages. On the one hand, this process enables to avoid metallurgical heterogeneities obtained by alternative bonding techniques. This was discussed by Kopp et al. (2004) and later by Merklein et al. (2012). On the other hand, roll bonding minimizes shrinkages and distortions at the bonding surface. A detailed description of the optimization process can be found in Groche and Schäfer (2007).

The application of plastic deformation for joining materials, as in the here considered process of roll bonding, reduces the post-processing operations and thus also the process costs which results in higher accuracy, reliability and environmental safety. The plastic deformation can be controlled by applying an optimal pressure. This results into mechanical joints which can be widely applied and are stronger than joints obtained by alternative joining techniques.

Cohesive zone elements were originally introduced by Dugdale (1960) and Barenblatt (1962) to predict crack propagation along interfaces. They are based on a traction-separation relation, which mirrors the fact that by increasing the interfacial separation, the traction across the interface reaches a maximum, then decreases and vanishes which goes along with a complete decohesion. This behavior can be seen in Tvergaard (1990) and Camacho and Ortiz (1996). Several other traction-separation laws were suggested by Chaboche et al. (2001) and Abdul-Baqi et al. (2005) for the modeling of cohesive zone elements. The main differences of the previously suggested cohesive zone models lie in the shape of the traction-separation curve and the mathematical relations that

* Corresponding author. Tel.: +49 0 241 80 25012; fax: +49 0 241 80 22001.

E-mail addresses: reza.kebriaei@rwth-aachen.de, rezakebriaei@gmail.com (R. Kebriaei).

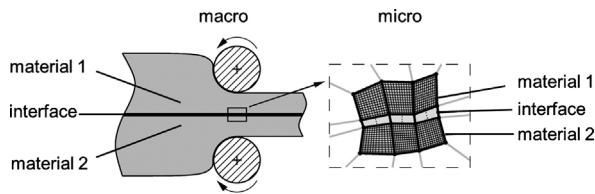


Fig. 1. Roll bonding.

describe that shape. Thermodynamically consistent cohesive zone elements for large deformations were introduced by Mergheim and Steinmann (2006) for isotropic materials and by Gasser and Holzapfel (2003) and Steinmann (2008) for anisotropic materials. Additionally, Mosler and Scheider (2011) developed a thermodynamically consistent cohesive zone element in which inelastic effects are taken into account. To the knowledge of the authors the previous studies were focused on cohesive zone models in the context of material separations at the interface, whereas no bonding effects are considered.

The present study deals with the multiscale modeling of the effects characterizing joining. The focus of the paper is on the mechanical characterization of the materials involved in the joining process, the interface topography and the numerical modeling of the interface. Following the earlier studies of Konchakova et al. (2010) and Paggi and Wriggers (2011), a cohesive zone element formulation for joining is developed. The cohesive zone law of Needleman (1990) is extended to be applicable to the cohesive interface in the joining process and to enable the evaluation of the bonding strength. In Section 2 the materials which are involved in the joining process are introduced. After that in Section 3, the element formulation which describes the cohesive behavior of the interface is discussed. The mechanical characterization of the involved materials is then subject of the first part of Section 4. This is followed by an investigation of the cohesive behavior of the interface. Finally, the application of the cohesive zone element formulation in the numerical simulation of the roll bonding process is presented.

2. Chemo-mechanical characterization

The aluminum alloys AA1050 and AA5754 are of high interest in industrial applications especially for joining processes due to their superior properties such as good corrosion resistance and high ductility. The chemical contents include iron, copper, nickel, manganese, chromium, magnesium, silicon, zinc and titanium and aluminum (see Table 1). The mechanical properties of the aluminum alloys AA1050 and AA5754 are investigated both at the macro and micro levels. The microstructures are observed by using scanning electron microscopy (SEM) and transmission electron microscopy (TEM).

The micromechanical characterization of the materials is done by means of a JSM 7000F field emission electron microscope. The microscope is equipped with a field emission gun (FEG) filament which offers a high resolution and permits characterization of the structures at the nano scale. The focused ion beam technique (FIB) is utilized since it represents an ideal tool for transmission electron microscope (TEM) sample preparation. This technique allows the application of electron-transparent foils for any region

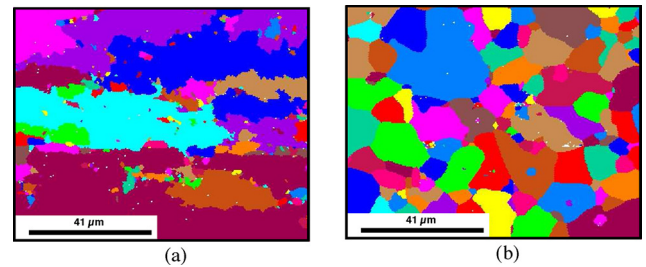


Fig. 2. Unique grain color map. If the point-to-point misorientation from grain to grain differs by more than 15° a different color is chosen: (a) AA1050 and (b) AA5754.

of the material under investigation. The ion milling process can be controlled by SEM which allows a better insight into the material. The analysis is performed using an electron beam with a size of less than 0.2 nm. Energy dispersive X-ray analysis (EDX), which is an x-ray technique used to identify the elemental composition of materials, is applied for finding the chemical compositions. The combination of TEM and EDX allows the mapping of the lateral distribution of elements with high spatial resolution.

Important texture information can be obtained by high resolution images and electron backscatter diffraction (EBSD) data. The combination of the information for the crystal structures and the chemical composition yields the complete characterization of the sample of interest. In Fig. 2, the crystallographic grain distribution for the two alloys under consideration is demonstrated by color mapping. If the point-to-point misorientation from grain to grain differs by more than 15° a different color is chosen. Obviously, AA1050 is characterized by a fine-grained texture, whereas large grains constitute the microstructure of AA5754.

Generally, the surfaces of the alloys are covered either by cover layers or films, such as e.g. oxide, chemical combinations remaining after pickling, absorbed moisture. During roll bonding, the cover layers are fractured due to the deformation of the base metal (here AA5754). Furthermore, micro cracks are developed in the virgin state of the base metal. The base metal extrudes through the micro cracks which meet the other surface (here AA1050). At this point joining begins (further details can be found in Wright et al., 1978). In this work, the sheet specimens are chosen in such a way that they have different rolling directions. This increases the bonding strength in the joining process.

There are two statistical distributions which are important for describing the structure of polycrystalline materials, namely the distribution of grains by crystallographic orientations (texture) and the distribution of grain boundaries by misorientations (grain boundary spectrum). The initial texture of the sample as generated directly from the measured EBSD data, is visualized in Fig. 3 in terms of 001, 011 and 111 pole figures. Alternatively, the EBSD data can be represented by means of orientation distribution functions (ODF). As an example, the representation of the ODF in the orientation space of the Euler angles for three different angles of 0° , 30° and 60° is illustrated in Fig. 4. The Euler angles describe the transformation from the reference frame of the sample into the crystallographic reference frame of each individual grain of the polycrystalline material.

The measured EBSD data, such as e.g. grain sizes and misorientations (see Fig. 2), crystallographic orientations (see Figs. 3 and 4),

Table 1
Chemical composition of the applied materials.

Material	Chemical composition									
	Fe	Cu	Ni	Mn	Cr	Mg	Si	Zn	Ti	Al
AA1050	0.3	0.05	0.0089	0.0094	0.0098	0.0187	0.09	0.0088	0.0177	bal
AA5754	0.21	0.01	–	0.26	0.02	3.08	0.08	0.02	0.0092	bal

Download English Version:

<https://daneshyari.com/en/article/790950>

Download Persian Version:

<https://daneshyari.com/article/790950>

[Daneshyari.com](https://daneshyari.com)